MAX-PLANCK-INSTITUT FÜR PLASMAPHYSIK

GARCHING BEI MÜNCHEN

Shape Optimization of Sharp Boundary Model Tokamaks with Elongated Cross-sections.

E. Rebhan[+)], A. Salat

IPP 6/170 March 1978

[+)] Institut für Theoretische Physik, University Düsseldorf,
4000 Düsseldorf

Die nachstehende Arbeit wurde im Rahmen des Vertrages zwischen dem Max-Planck-Institut für Plasmaphysik und der Europäischen Atomgemeinschaft über die Zusammenarbeit auf dem Gebiete der Plasmaphysik durchgeführt.

6/170 E. Rebhan, A. Salat

Shape Optimization of Sharp Boundary Model Tokamaks with Elongated Cross-sections.

March 1978 (in English

Abstract

Using a modified method of steepest descent in a multidimensional space of Fourier coefficients which represent the plasma boundary, the critical beta of sharp boundary model tokamaks is maximized for fixed values of aspect ratio and poloidal beta under the constraint that the plasma be stable with respect to axisymmetric MHD modes. In the subclass of elliptical cross-sections it is demonstrated that the omission of nonaxisymmetric stability is of minor influence for the determination of the optimum shape. Since for small aspect ratio there is a preference for doublet type shapes, a theory of axisymmetric stability for sharp boundary doublets is included in the paper.

Introduction

It is well known that in tokamak equilibria ß can be increased by using vertically elongated plasma cross-sections. Generally, the relation between ß and the plasma elongation is even monotonic, and the benefits of this relation are only restricted by stability. Unfortunately, owing to axisymmetric MHD instabilities [1,2], there is a rather small upper limit for the plasma elongation which allows a moderate improvement in ß for small aspect ratio only.

However, ß depends not only on elongation but also on other details of the plasma shape such as ellipticity, triangularity etc., and furthermore it is strongly influenced by the current distribution.

An optimal optimization of a tokamak would maximize ß by adjusting the plasma shape as well as the current distribution, thereby observing some constructive and technical restrictions and observing the constraint that the plasma be stable with respect to all possible plasma instabilities, ideal and non-ideal, axisymmetric and nonaxisymmetric. Apart from the supposition that this problem would have no solution, it is in any case far beyond the scope of present-day possibilities. One is thus forced to settle for less ambitious objectives and still hope to obtain results showing the correct trend.

In this paper a constant pressure sharp boundary tokamak model is used to determine a plasma shape which, on the one hand, causes the highest possible ß -values and, on the other, is still stable with respect to axisymmetric MHD modes. In this choice of plasma model only the influence of the plasma shape may be used for maximizing ß, the equally important current distribution not being variable. Furthermore, we have not included wall stabilization since with fixed external walls the optimum shape would depend too strongly on the wall shape. In addition, a simultaneous optimization of the wall shape would at least double the parameters of the problem. Nevertheless, inclusion of wall stabilization would appear as a rewarding ingredient.

Regarding the omission of nonaxisymmetric modes, we believe that at least for the surface current model (SCM) the optimum shape (the shape for which ß becomes maximum and the plasma is still MHD stable) is determined much more strongly by axisymmetric than by nonaxisymmetric stability. One argument in favour of this opinion is that for the SCM each plasma shape is stable with respect to nonaxisymmetric modes if only q is chosen large enough, while stability with respect to axisymmetric modes cannot be achieved by any choice of q unless the plasma shape is chosen properly (Ref. [1]). An even stronger argument results from considering elliptical plasma cross-sections. Figure 1 shows the maximum ß compatible with nonaxisymmetric stability as a function of the plasma elongation according to Ref. [3]. Also shown is the region which is stable with respect

to axisymmetric modes calculated according to Ref. [2]. Only the shaded area is stable with respect to both axisymmetric and nonaxisymmetric modes, and it becomes obvious from this diagram that the optimum elongation is essentially determined by the boundary for axisymmetric stability, while the maximum achievable of ß, or, according to eqs. (1.2) - (1.3) in section I, equivalently the critical safety factor q, is essentially determined by nonaxisymmetric stability.

In the literature there have already been attempts to maximize ß by adjusting the plasma shape, see e.g. [4] [5]. However, firstly most of them were restricted to nonaxisymmetric modes and the severe restrictions coming from axisymmetric modes according to Fig. 1 were thus not included. Secondly, the optimization was performed in a very restricted class of shapes. In our paper we admit a quite general plasma shape and, starting with a stable shape of relatively low ß, we maximize by a modified steepest descent method in a space of Fourier parameters which determine the plasma shape. Thus, no preconception of the optimum plasma shape is contained. This method forces us to calculate the stability of very many rather different looking equilibria, a process for which the surface current model is especially suitable since the stability problem can be reduced to a one-dimensional numerical problem on the plasma boundary and since the computer time for calculating the stability of one specific equilibrium is fairly short.

The high flexibility of the SCM is paid for with a rather exotic current distribution, and the question of the relevance of the corresponding stability results arises. Restricting the discussion to axisymmetric stability, we note that according to our results in Refs. [1,2] for simple plasma cross-sections such as ellipses etc. at infinite aspect ratio exactly the same stability boundaries are obtained as for a diffuse current model (DCM). For small A, the perturbations which minimize $\delta^2 W$ for the SCM are found to be nonlocal external gross modes, for which the details of the current distribution are of minor importance, and the SCM may therefore be expected to be a similarly good approximation to reality as it is known to be for stability with respect to the nonaxisymmetric m = n = 1 gross mode. Recent numerical studies of axisymmetric modes for diffused current models [6] show an excellent qualitative agreement with our SCM calculations. Thus, we may expect results which are qualitatively correct, and the SCM appears as a useful guide through parameter space.

The paper is arranged as follows: in Sec. I we summarize the equilibrium properties of the SCM as needed in this paper and discuss the representation of the plasma shape together with an appropriate coordinate system. Since in the course of optimization doublet-type shapes come up, certain specific problems arising in the stability theory of axisymmetric modes for doublet shapes are treated in Sec. II. In Sec. III, the method of optimization is discussed, and in Sec. IV numerical results are presented.

I. Equilibrium properties and representation of the plasma boundary

We use cylindrical coordinates R, θ, z and dimensionless quantities as introduced in Refs. [1] and [2]. The aspect ratio A will be defined by

$$R_{max} = 1 + 1/A \quad , \qquad R_{min} = 1 - 1/A \quad , \tag{1.1}$$

the middle of the plasma thus being located at R = 1 (see Fig. 2). For the poloidal equilibrium magnetic field on the plasma boundary, we have

$$B = \frac{1}{R} \left[1 + \beta_p (R^2 - 1) \right]^{1/2} \quad , \tag{1.2}$$

where β_p is related to the plasma pressure and the poloidal field $B_o = 1$ at R = 1 by $\beta_p = 2p/B_o^2$. With the usual integral definition of the safety factor q we use the β -definition $\beta = p/(p + \frac{B^2}{2}p1\Big|_{R=1})$ and have the relation

$$\beta = \beta_p/(1 + A^2 q^2/q_g^2) \quad , \tag{1.3}$$

where

$$q_g = \frac{A}{2\pi} \oint \frac{dl}{R^2 B} \quad , \tag{1.4}$$

the integration extending over a poloidal cut of the plasma surface. β_p is restricted to values

$$\beta_p \leq \beta_p^* = A^2/(2A - 1). \tag{1.5}$$

Instead of ß we shall also use the parameter

$$\alpha^2 = \frac{6}{5}\,(1 - ß)/ß. \tag{1.6}$$

We note that our definitions of ß and $ß_p$ use magnetic field quantities in the middle between R_{max} and R_{min}, while averages over the plasma surface are also frequently used. Especially in an optimization procedure, this may lead to slight differences which, however, appear to be unimportant in view of the approximate character of the SCM. On the other hand, our definition allows of more explicit equilibrium relations, a fact which proves to be an important advantage, especially in the numerical optimization procedure.

To describe the plasma boundary we introduce polar coordinates s, u in the θ = const planes as shown in Fig. 2 and consider only plasma boundaries which are symmetric with respect to the equatorial plane z = 0. Using a Fourier representation, we thus have

$$s = s(u) = \sum_{n=0}^{N} a_n \cos n\,u + \ldots\ldots \tag{1.7}$$

and

$$R = 1 + s(u) \cdot \cos u \ ,$$

where in our numerical procedure only a finite number of coefficients is taken along. Although a good approximation of an arbitrarily given boundary may require a relatively large number of Fourier coefficients, it turned out in our optimization procedure that for $N \simeq 10$ an increase of N leaves the optimum value of ß practically unchanged.

Apparently, multiplication of a curve s(u) with a constant λ leads to another curve $s_\lambda(u) = \lambda s(u)$, which has the same shape properties as s(u) and differs only in aspect ratio. We used this by rewriting

$$s(u) = c \cdot \left[1 + \sum_{n=1}^{N} c_n \cos n u \right], \tag{1.8}$$

where now the coefficients $c_1, \ldots c_N$ determine the specific shape, while c determines A.

According to eqs. (1.1) and (1.8) we must have

$$\text{Max} \left[(1 + \sum_{n=1}^{N} c_n \cos n u) \cos u \right] = - \text{Min} \left[(1 + \sum_{n=1}^{N} c_n \cos n u) \cdot \cos u \right] \tag{1.9}$$

and hence one of the coefficients $c_1, \ldots, c_N$ is dependent on the others. For $c_1, \ldots, c_N$ given and with eq. (1.9) being satisfied, c is related to A by, for instance,

$$\frac{1}{A} = c \cdot \text{Max} \left[(1 + \sum_{n=1}^{N} c_n \cos n u) \cos u \right] \tag{1.10}$$

In our numerical calculations, instead of the polar coordinate u we have used an "adapted" coordinate v on the plasma boundary, which is related to u by

$$v = 2\pi \frac{\int_0^{l(u)} \sqrt{1 + \kappa^2/A^2}\, dl}{\oint \sqrt{1 + \kappa^2/A^2}\, dl}, \tag{1.11}$$

where $\kappa(u)$ is the curvature of the curve defined by the plasma boundary in the θ = const plane, and l(u) the arc length of it measured from u = 0. Since dv/dl is essentially proportional

to κ, for constant stepsize Δv the numerical grid points become denser at boundary sections with large curvature than on those with small curvature. With these adapted coordinates, much faster numerical convergence for noncircular plasma cross-sections was obtained than with polar coordinates.

II. Axisymmetric stability of doublet-type equilibria

In our paper on the stability of sharp-boundary tokamaks with respect to general axisymmetric modes [2] we restricted our consideration to plasma cross-sections $z = z(R)$ for which $z(R)$ is a single-valued function for $z \geq 0$ and $z \leq 0$. In doublet-type configurations as shown in Fig. 2 this assumption is no longer valid, and since in the procedure of optimization at low aspect ratio there is a preference for doublets, we must develop a stability theory for these. According to Ref. [2], in $\delta^2 W = \delta W_{pl} + \delta W_S + \delta W_v$ the multivaluedness of $z(R)$ affects only δW_{pl}, while δW_S and δW_v may be calculated as for single-valued functions $z(R)$. Thus, we shall consider her only the minimization of δW_{pl}, which is given by eq. (3.7) in Ref. [2],

$$\delta W_{pl} = \frac{5}{6} \pi \beta_p \int \left[R\left(\xi_R + \eta_z + \frac{\xi}{R}\right)^2 + \frac{\alpha^2}{R} \left(\xi_R + \eta_z - \frac{\xi}{R}\right)^2 \right] d R \, dz \tag{2.1}$$

$$= W(\xi, \eta) ,$$

where ξ and η are the x and z components of the perturbation, and $\xi_R = \frac{d\xi}{dR}$, etc. If we split ξ and η into contributions which are symmetric and antisymmetric with respect to the $z = 0$ plane:

$$\xi = \xi^s + \xi^a , \qquad \eta = \eta^s + \eta^a ,$$

where $\xi^s(R, -z) = \xi^s(R,z)$, $\xi^a(R, -z) = -\xi^a(R,z)$ etc., then δW_{pl} separates into two independent contributions

$$\delta W_{pl} = W(\xi^s, \eta^a) + W(\xi^a, \eta^s). \tag{2.2}$$

Now, δW_{pl} must be minimized with respect to ξ and η for given

$$\xi_n = \underline{n} \cdot \underline{\xi} = n_R \xi + n_z \eta \quad ,$$

where the vector $\underline{n}$ with R-component n_R and z-component n_z is the normal vector on the plasma surface. Since

$$n_R \xi^s + n_z \eta^a = \xi_n^s \quad , \tag{2.3a}$$

$$n_R \xi^a + n_z \eta^s = \xi_n^a \quad , \tag{2.3b}$$

we shall denote

$$\delta W_{pl}^s = W(\xi^s, \eta^a), \quad \delta W_{pl}^a = W(\xi^a, \eta^s), \tag{2.4}$$

where in the minimization of δW_{pl}^s and δW_{pl}^a we must prescribe on the boundary the values of ξ_n^s and ξ_n^a respectively.

In the R,z -plane, we shall divide the plasma interior into the regions $R_{min} \leq R \leq R_1$ and $R_r \leq R \leq R_{max}$, which we call "doublet regions", and the region $R_1 \leq R \leq R_r$, which we call non-doublet region (see Fig.2). As in Ref. [2], the variation of δW_{pl} (eq.(2.1)) yields the Euler equations

$$\begin{aligned} &(\xi_R + \eta_z)_R + \frac{R^2 - \alpha^2}{R^2 + \alpha^2} \left(\frac{\xi}{R}\right)_R = 0 \quad , \\ &(\xi_R + \eta_z + \frac{R^2 - \alpha^2}{R^2 + \alpha^2} \frac{\xi}{R})_z = 0 \quad , \end{aligned} \tag{2.5}$$

with the general solution

$$\xi = \frac{\gamma^2(R)}{4} f'(R) , \tag{2.6a}$$

$$\eta = h(R)z + g(R) , \tag{2.6b}$$

where the abbreviations

$$\gamma(R) = \frac{\alpha^2 + R^2}{\alpha} \tag{2.7}$$

and

$$h(R) = \frac{\gamma^2}{4} \left[- f'' + \frac{\alpha^2 - 5R^2}{R\gamma\alpha} f' + \frac{4}{\gamma 2} f \right] \tag{2.8}$$

are used, and where f and g are arbitrary functions of R. In dealing with δW^s_{pl} and δW^a_{pl}, according to eqs. (2.4) we have to single out solutions with appropriate symmetry properties. Since these symmetry requirements have different consequences for the non-doublet region and doublet region (s) (the latter may amount to one or two), we shall treat the regions separately. Let us first consider the non-doublet region $R_l \leq R \leq R_r$. There, the plasma above z = 0 is connected with the plasma below, and from eqs. (2.6) we obviously obtain

$$\xi^a \equiv 0 \quad , \quad \eta^s = g(R) \quad , \tag{2.9}$$

$$\xi^s = \frac{\gamma^2(R)}{4} f'(R), \ \eta^a = h(R)z . \tag{2.10}$$

These Euler solutions must be inserted in the conditions (2.3) on the plasma boundary. Introducing the arc length l on the boundary z = z(R), with the notations f(l) = f(R(l)), $\dot{f}$ = df/dl etc. and using

$$n_R = \dot{z} \quad , \quad n_z = - \dot{R} \quad , \tag{2.11}$$

we obtain after a little calculation

$$g = \xi_n^a / n_z \tag{2.12}$$

and

$$\ddot{f} + \left(\frac{5\,R^2 - \alpha^2}{\alpha\,\gamma} \frac{\dot{R}}{R} - \frac{\ddot{R}}{\dot{R}} + \frac{\dot{z}}{z} \right) \dot{f} - \frac{4\dot{R}^2}{\gamma^2} f = \frac{4\dot{R}}{\gamma^2 z} \xi_n^s \quad . \tag{2.13a}$$

For uniformity in the case $\xi_n = \xi_n^a$ underlying eqs.(2.9) we introduce a function

$$f(1) \equiv 0 \tag{2.13b}$$

and formally keep eq.(2.6a).

According to the definition of the non-doublet region, n_z nowhere vanishes and thus eq. (2.12) everywhere defines a unique function g(R). We shall discuss the problem of appropriate boundary conditions for eq. (2.13a) in connection with the corresponding problem for the doublet region (s).

Let us now turn to the doublet region (s). There, except for $R = R_l$ and/or $R = R_r$, the Euler solutions ξ and η may differ above and below z = 0 since the plasma regions are disconnected. Perturbations, which in each separate plasma region are Euler solutions, are given by

$$\xi^a = \frac{\gamma^2}{4} f'(R) \cdot \operatorname{sign} z \quad \text{with } f'(R_l) = f'(R_r) = 0, \tag{2.14a}$$

$$\eta^s = h(R)\, z \cdot \operatorname{sign} z + g(R) \quad , \tag{2.14b}$$

$$\xi^s = \frac{\gamma^2}{4} f'(R) \quad , \tag{2.15a}$$

$$\eta^a = h(R) z + g(R) \cdot \operatorname{sign} z \text{ with } g(R_l) = g(R_r) = 0 \quad . \tag{2.15b}$$

The additional conditions in eqs. (2.14a) and (2.15b) take care of the symmetry requirements at the endpoints of the doublet region(s) and in Appendix A they are shown to be automatically satisfied on the assumption $\ddot{R} \neq 0$ at $z = 0$, $R = R_l$ and/or $R = R_r$. Since the pairs ξ^a, η^s and ξ^s, η^a are independent, in eqs. (2.14) and (2.15) different functions f(R), g(R) may occur; we have used the same notation just for convenience.

We again determine f(R) and g(R) by inserting eqs.(2.14) - (2.15) in the conditions (2.3) and restrict ourselves to the region $z \geq 0$. There, for given R a condition arises at two boundary points P and $\hat{P}$ (see Fig. 2) since for each point P on the doublet boundary there exists a "conjugate" point $\hat{P}$. Marking all quantities at conjugate points with $\hat{}$ and omitting the superscripts ^{s} and ^{a} we obtain at P and $\hat{P}$ respectively the quations

$$\frac{\gamma^2}{4}\, n_R\, f' + n_z (h\, z + g) = \xi_n \,, \tag{2.16}$$

$$\frac{\gamma^2}{4}\, \hat{n}_R\, f' + \hat{n}_z (h\, \hat{z} + g) = \hat{\xi}_n \,. \tag{2.17}$$

Multiplying eq. (2.16) by $\hat{n}_z$ $\hat{z}$, and eq. (2.17) by n_z z, and substracting the two yields

$$g(R) = \frac{1}{(\hat{z}-z)} \left[\frac{z}{n_z} (\hat{\xi}_n - \frac{\gamma^2}{4}\, \hat{n}_R\, f') - \frac{\hat{z}}{n_z} (\xi_n - \frac{\gamma^2}{4}\, n_R\, F') \right]. \tag{2.18}$$

Once f(R) is determined, g(R) is also given.

Turning to the determination of f, we multiply eq. (2.16) by $\hat{n}_z$, eq. (2.17) by n_z, substract both, and after a little calculation, switching from the variable R to 1 using eqs. (2.11), we obtain

$$\ddot{f} + \left(\frac{5R^2-\alpha^2}{\alpha\gamma}\,\frac{\dot{R}}{R} - \frac{\ddot{R}}{\dot{R}} + \frac{(\dot{z}\hat{\dot{R}} - \hat{\dot{z}}\dot{R})}{\hat{\dot{R}}(z-\hat{z})}\right)\dot{f} - \frac{4\dot{R}^2}{\gamma^2}\,f = \frac{4\dot{R}}{\gamma^2\hat{\dot{R}}}\,\frac{(\xi_n\hat{\dot{R}} - \hat{\xi}_n\dot{R})}{(z-\hat{z})} \quad . \tag{2.19}$$

We shall now discuss the boundary conditions to be imposed on the differential eqs. (2.13) and (2.19). On the plasma boundary, firstly at the two points where $R = R_{min}$ and $R = R_{max}$ and secondly at the point(s) $z = 0$, $R = R_l$ and/or $R = R_r$, we have $\dot{R} = 0$, $n_R = 1$, $n_z = 0$, and with $\xi = \underline{n} \cdot \underline{\xi} = \xi_n$ and eq. (2.6a) we obtain

$$\dot{f} = \frac{4}{\gamma^2}\,\xi_n\,\dot{R} = 0 \quad . \tag{2.20}$$

It is immediately seen from eq. (2.19) that at the second mentioned point(s), because of $\dot{R} = 0$ in the denominator of the $\dot{f}$-coefficient, eq. (2.20) is automatically satisfied for each solution f(1). Thus, there remain two real boundary conditions (2.20) at R_{min} and R_{max}, and they must still hold if only one doublet region exists and either R_{min} or R_{max} is reached at $z = 0$ in the non-doublet region.

Further boundary conditions result from the requirement that δW_{pl} become a minimum. Since δW_{pl} contains the R-derivative of ξ, eq. (2.1), a discontinuity of ξ in the R-direction would blow up δW_{pl} to an infinite value, and to avoid this, according to eq. (2.6)

together with ξ also $f'(R) = \dot{f}(1)/\dot{R}(1)$ and $\dot{f}(1)$ must be equal at the connecting endpoint(s) of non-doublet and doublet region(s). It is shown in Appendix B that the Euler solutions (2.9), (2.10) and (2.15), (2.16) actually minimize δW_{pl}, if in addition there is equality also for f(1). We note that the continuity requirement for f and $\dot{f}$ is not self-evident. Firstly, in the transition from non-doublet to doublet regions some of the coefficients in the differential equation for f are discontinuous. Secondly, after continuity of f and $\dot{f}$ is imposed, $\ddot{f}$ and hence, according to eqs. (2.6b) and (2.8), also the z-component η of the perturbation will in general be discontinuous. To summarize, the number of conditions on the boundary now obtained is twice the number of independent differential equations, and it is shown in Appendix B that unique solutions f(1) thus exist which define single -valued functions f(R) = f(1(R)). Furthermore, it is shown that for given $\xi_n^{s,a}$ (1) the minimum of $\delta W_{pl}^{s,a}$ is given by a contour integral over the plasma boundary,

$$\text{Min } \delta W_{pl}^{s,a} = \frac{5}{6}\pi\beta_p \oint \frac{R^2 + \alpha^2}{R} f(1)\, \xi_n^{s,a}(1)\, d1. \qquad (2.21)$$

The numerical evaluation of Min $\delta W_{pl}^{s,a}$ requires the solution of boundary value problems for ordinary second order differential equations and a contour integration. Standard methods are applicable, for both purposes, the use of the adapted coordinates of Section I speeding up numerical convergence. As for convex plasma cross-sections, the essential step is then, after adding the contributions δW_s and δW_v, to minimize $\delta^2 W$ with respect to ξ_n^s and ξ_n^a. All this can be carried out completely by analogy with Refs. [1] and [2], and

the minimum of $\delta^2 W$ thus obtained will be denoted by

$$W_{min} = \text{Min } (\delta^2 W) \quad . \tag{2.22}$$

For a typical doublet type cross-section with symmetry around the R = 1 line we show the antisymmetric minimizing perurbation in Fig. 3. The instability in Fig. 3 is a (discontinuous) vertical downshift combined with a constriction of the upper doublet wings which makes it easier for the plasma to slip through the toroidal current loops needed close to the plasma in the z = 0 plane in order to create the waist of the equilibrium shape.

If for doublet-type equilibria the stability boundary is calculated by minimizing $\delta^2 W$ in the subset of slip-mode perturbations, Ref. [1], which by definition are q-independent, almost exactly the same result is obtained as with full minimization. Thus, the almost complete independence of axisymmetric stability on q observed earlier at convex plasma cross-sections, Ref. [2], transfers to doublet type cross-sections.

III. Optimization of the plasma boundary

According to the theory of equilibrium as presented in Section I, the quantities q, β_p, A and the shape determining Fourier coefficients $c_1, \ldots, c_N$ in eq. (1.7) are, with one exception, independent parameters. From eq. (1.2) we conclude that in order to obtain large β, the independent quantities A and q should be small, β_p should be large, and the dependent quantity q_g should be large. β depends on the plasma shape through q_g, which for given A obviously increases with the circumference of the plasma cross-section and particularly with the vertical elongation.

In a given experimental set there are structural restrictions on $1/A$ and practical limits on β_p, and in a planned experiment any lessening of these restrictions is limited by economical constraints. Therefore, it appears reasonable to keep both quantities fixed during optimization. With fixed A the parameter c in eq. (1.8) becomes a dependent variable, and we choose c_1 as another dependent variable in order to satisfy condition (1.9). Since for fixed other parameters β is numerically found to vary monotonically with c_2, it is convenient to employ c_2 as a dependent variable for the adjustment of β during the optimization.

For given aspect ratio, the optimization leads to vertically elongated cross-sections, and since for these the q dependence of the boundaries for axisymmetric stability is especially weak (for convex shapes there is no dependence at all; see Ref. [2]), we

also chose q as a fixed parameter, and we arbitrarily chose q = 1. With this choice we cannot expect to obtain the correct optimum values of ß, but according to our considerations in the introduction we may expect a good approximation to the optimum plasma shape.

The physical problem of finding a configuration with maximum ß which is still stable with respect to axisymmetric modes is mathematically the problem of finding the maximum or supremum of a function of very many variables under the constraint $W_{min} \geq 0$. This is known to be a hard problem, and the method of steepest descent would present itself as a useful tool. However, the existence of several unstable modes may make W_{min} a nonanalytical function of the equilibrium parameters, and particularly this function is not given directly but in a highly implicit manner. There are thus very inconvenient obstacles to applying this method, and we therefore developed a modification which we shall now describe.

According to the foregoing we have the following classification of variables: A, $ß_p$ and q are prescribed quantities, c_3, c_4, ..., c_N are the free variables of the problem, c, c_1 and c_2 are dependent variables, and ß is the quantity to be maximized by variation of the free variables c_3, ..., c_N.

Our optimization procedure starts with a circular cross-section, i.e. $c_1 = c_2 = ... = c_N = 0$, a configuration which according to Ref. [2] is stable, $W_{min} > 0$. Then, with unaltered c_3, ..., c_N we increase ß stepwise with appropriate readjustment of c, c_1 and c_2 until $W_{min} < 0$.

Next, with the last value of ß fixed, we try to bring W_{min} back to a positive value. This is done by changing c_3, c_4.... one after the other such that W_{min} assumes a relative maximum with respect to the variable whose turn it is. Numerically, this was accomplished by a stepwise increase or decrease of the variable whose turn it is, with ever growing stepsize for increasing W_{min} and with a return to the starting stepsize after a change of direction due to decreasing W_{min} . Generally, the maximizing property of a c_i gets lost after its turn is past and therefore after c_N the procedure is restarted with c_3. As soon as a positive value of W_{min} is reached, we interrupt the variation of the independent variables and, fixing their last values, we again increase ß stepwise with appropriate readjustment of c, c_1 and c_2 until $W_{min} < 0$. Then the variation of the c_3, ..., c_N is resumed as above. In this way ß increases step by step, and with given minimum stepsize of the several operations the whole procedure ends after a finite number of steps. W_{min} then assumes approximately a relative maximum with respect to all free variables simultaneously and is still negative. Going back to the last ß with positive W_{min} the procedure is restarted with smaller size of the several minimum steps until a desired accuracy is reached and the parameters corresponding to the last positive W_{min} can be used as optimum parameters.

In Fig. 4 our method is graphically illustrated by a two-dimensional analogue.

IV Numerical results

It is clear from the last section that in order to obtain an optimum plasma shape, the stability of very many intermediate configurations must be calculated. The numerical methods for calculating the stability of each specific one of them have been presented in Ref. [2], modifications due to the occurrence of doublet-type cross-sections are described in Section II, and the methods for obtaining an optimum shape are found in Section III.

Figures 5a) and 5b) show the optimum shapes which we obtained with $q = 1$, $\beta_p = 1$ and $\beta_p = 2$, respectively, for different values of A. For each optimum shape the maximum property of W_{min} with respect to all of the free variables simultaneously was tested, and one of the tests is shown in Fig. 6. For large A the optimum shapes are almost circles. With decreasing A gradually a preference for straight vertical sections develops which are a little longer on the side near the axis of symmetry, the optimum configurations thus looking like a combination of racetrack and D-shape. This kind of optimum shape varies continuously with A and gets more and more pronounced with decreasing A until at $A^* \approx 3.8$ for $\beta_p = 1$ and $A^* \approx 5.9$ for $\beta_p = 2$ a sudden qualitative change occurs: if A is only slightly below A^*, in the process of optimization a constriction of the plasma boundary develops forming a doublet-like plasma shape. With constantly increasing β this constriction becomes tighter and tighter until finally a stage is reached where we can no longer trust the

accuracy of our code since near z = 0 the curvature of the boundary becomes too large. It thus cannot be decided whether the optimization procedure comes to an end at a certain very constricted doublet shape or goes on trying to tear the plasma into two separate tori. In the case $A < A^*$ we have therefore shown intermediate shapes in Figs. 7a), b) for which we can still trust our code. In addition, for $A > A^*$ we also started with constricted shapes and observed that the constriction was gradually reduced in a subsequent optimization until the same optimum shape was obtained as when starting from a circular shape. This indicates that no obvious bifurcation is present, although bifurcation generally cannot be excluded in this way. The shapes shown in Figs. 5 and 7 were obtained with between 10 and 12 Fourier coefficients (c, c_1 and c_2 being included in the account). A further increase of their number brought no visible change in the optimum shape. In Table 1 we have listed the values of c and c_1, ..., c_8 for $\beta_p = 1$ and several values of A, which allows reconstruction of the optimum shapes and the indented shapes with $A < A^*$ of Fig. 7a with sufficient accuracy.

Since we have arbitrarily chosen q = 1 and not considered nonaxisymmetric stability we cannot expect the optimum values of β to be accurate. We have therefore only calculated the enhancement of β as compared with the β value of a circular cross-section at q = 1 and present the results in Fig. 8. (The small circles and crosses below $A = A^*$ indicate the β values of intermediate doublet shapes). Since the β enhancement changes only slightly when a larger but still equal value of q is chosen for both the circular and optimum shapes, the curves in Fig. 8 will only need a marked down-correction if

in the transition from circular shape to optimum shape after inclusion of nonaxisymmetric modes q must appreciably be increased. For comparison we have shown in Fig. 9 ($\beta_p = 1$, $q = 1$) the enhancement of β which can be obtained with elongated ellipses.

Conclusions

Employing a modified method of steepest descent in a space of Fourier coefficients which determine the plasma boundary we maximized ß for fixed values of A, $ß_p$ and q under the constraint that stability with respect to axisymmetric perturbations is observed. Thereby q was fixed only for convenience in spite of the far reaching q independence of axisymmetric stability. Although nonaxisymmetric stability was excluded, we expect rather reliable results for the optimum plasma shape but less reliable for the maximum ß.

It turned out that for large A only very small deviations from circular shape are possible, that for decreasing A the optimum shape is a superposition of racetrack and D-shape, and that below a $ß_p$-dependent threshold A^* (e.g. $A^* \approx 3.8$ for $ß_p = 1$ and $A^* \approx 5.9$ for $ß_p = 2$) doublet-type shapes are preferable. Across this threshold the optimum shape is a discontinuous function of A such that below it the optimization procedure went on producing higher and higher ß with more and more constricted stable doublet shapes until it had to be stopped because of numerical accuracy problems. Down to A^* the gain in ß by shaping the plasma increases monotonically with decreasing A and increases with $ß_p$ for fixed A. Across the threshold A^* it jumps to much higher values, and it thus appears rewarding to fall below this threshold.

Acknowledgement:

One of the authors (E.R.) expresses his gratitude to Max-Planck-Institut für Plasmaphysik for hospitality on several occasions while finishing the paper. Most of this work was already completed while he was still a member of Institut für Plasmaphysik.

Appendix A

We consider the boundary line(s) $R = R_l$ and/or $R = R_r$. With $\dot{f}(1) = f'(R)\,\dot{R}(1)$ the eqs. (B10) from Appendix B may be written in the form

$$f'(R_l) = \frac{4}{\gamma^2}\,\xi_n(R_l,0), \qquad f'(R_r) = \frac{4}{\gamma^2}\,\xi_n(R_r,0). \tag{A1}$$

Because of $\xi_n^a(R_l,0)$ (=) $\xi_n^a(R_r,0) = 0$ the condition(s) in eq. (2.14a) is (are) thus automatically satisfied.

From eq. (2.18) we obtain there

$$g = (\xi_n - \frac{\gamma^2}{4}\,n_R\,f')/n_z \quad . \tag{A2}$$

According to (A1) with $n_R(R_l,0)$ (=) $n_R(R_r,0) = 0$, both nominator and denominator vanish. With $n_z = -\dot{R}$ we therefore get

$$g = -\frac{d}{dl}\,(\xi_n - \frac{\gamma^2}{4}\,n_R\,f')/\ddot{R} \quad . \tag{A3}$$

For $\xi_n = \xi_n^s$ the bracket is a symmetric function of l, its derivative vanishes and on the assumption that $\ddot{R} \neq 0$ condition(s) (2.15b) is (are) automatically satisfied.

Appendix B

We shall first show in subsection a) that the Euler solutions minimize $\delta^2 W$, assuming unique existence and single-valuedness. These are proven afterwards in subsection b).

a) let $\underline{\xi}^o$ (R,z) be the vector function made up by the Euler solutions (2.9), (2.10) and (2.14), (2.15) in the different subregions of the plasma, and let $\underline{\xi} = \underline{\xi}^o + \underline{\xi}^1$ be an arbitrary perturbation which satisfies $\underline{n} \cdot \underline{\xi} = \underline{n} \cdot \underline{\xi}^o = \xi_n$ so that

$$\underline{n} \cdot \underline{\xi}^1 = n_R \xi^1 + n_z \eta^1 = 0. \tag{B1}$$

With the notation of eq. (2.1) we have

$$\delta W_{pl} = W(\xi^o, \eta^o) + W(\xi^1, \eta^1) + W^{o1} , \tag{B2}$$

where

$$\frac{1}{2} W^{o1} = \frac{5}{6} \pi \beta_p \int \Big[R(\xi^1_R + \eta^1_z + \frac{\xi^1}{R})(\xi^o_R + \eta^o_z + \frac{\xi^o}{R})$$

$$+ \frac{\alpha^2}{R} (\xi^1_R + \eta^1_z - \frac{\xi^1}{R}) \; (\xi^o_R + \eta^o_z - \frac{\xi^o}{R}) \Big] \, dRdz. \tag{B3}$$

Using the Euler equation for $\underline{\xi}^o$, we should like to integrate this by parts. However, since η^o and ξ^o_R are discontinuous across the separation line(s), in the strips $R_1 - \varepsilon \leq R \leq R_1 + \varepsilon$ and/or $R_r - \varepsilon \leq R \leq R_r + \varepsilon$ the integrand is left as it stands, and because it is finite although discontinuous, there is no contribution from the strip(s) to W^{o1} in the limit $\varepsilon \to 0$. From the remaining subregions we then obtain, after partial integration and use of the Euler equations (2.5),

$$\frac{1}{2}W^{o1} = \frac{5}{6}\pi\beta_p \sum\int \{ \frac{\partial}{\partial R}\left[R\xi^1(\xi_R^o + \eta_z^o + \frac{\xi^o}{R}) + \frac{\alpha^2}{R}\xi^1(\xi_R^o + \eta_z^o - \frac{\xi^o}{R})\right]$$

$$+ \frac{\partial}{\partial z}\left[R\eta^1(\xi_R^o + \eta_z^o + \frac{\xi^o}{R}) + \frac{\alpha^2}{R}\eta^1(\xi_R^o + \eta_z^o - \frac{\xi^o}{R})\right]\} \, dRdz$$

$$= \frac{5}{6}\pi\beta_p \sum \oint (\underline{n}\cdot\underline{\xi}^1)\left[R(\xi_R^o + \eta_z^o + \frac{\xi^o}{R}) + \frac{\alpha^2}{R}(\xi_R^o + \eta_z^o - \frac{\xi^o}{R})\right] dl. \tag{B4}$$

Insertion of the Euler solutions (2.6) yields

$$\frac{1}{2}W^{o1} = \frac{5}{6}\pi\beta_p \sum \oint (\underline{n}\cdot\underline{\xi}^1)\,\frac{\alpha^2+R^2}{R}\,f \quad dl. \tag{B5}$$

The sum contains separate contributions from the different subregions, the line integrals extending over the closed contours formed by separation line(s) and sections of the plasma boundary. The contributions of the latter vanish because of eq. (B1) while each separation line contributes twice, one contribution with $n_R = -1$ coming from the right and a second with $n_R = 1$ coming from the left adjacent region. Finally, since across the separation line(s) with ξ also ξ^1 must be continuous and since alongside $R = \text{const}$, $n_z = 0$ and $dl = dz$

$$\frac{W^{o1}}{2} = -\frac{5}{6}\pi\beta_p\left[\frac{\alpha^2+R_1^2}{R_1}\int_{z_1 min}^{z_1 max} \Delta f_1\,\xi^1(R_1,z)\,dz \;(+)\; \frac{\alpha^2+R_r^2}{R_r}\int_{z_r min}^{z_r max} \Delta f_r\,\xi^1(R_r,z)\,dz\right], \tag{B6}$$

where, for example,

$$\Delta f_r = \lim_{\varepsilon \to o} \left[f(R_r + \varepsilon) - f(R_r - \varepsilon) \right]. \tag{B7}$$

The case $\xi_n = \xi_n^a$, which according to eqs. (2.1), (2.4) and (2.9) should have no contribution from the non-doublet region, is properly included by means of the convention (2.13b).

Since according to its definition $W(\xi^1, \eta^1) \geq 0$, it is readily seen from eq. (B2) that for

$$\Delta f_1 = 0 \text{ and/or } \Delta f_r = 0 \tag{B8}$$

because of $W^{o1} = 0$ the minimum of δW_{p1} is achieved if $\underline{\xi}_1 = 0$, i.e. $\underline{\xi} = \underline{\xi}_o$. Since $\text{Min}\delta W_{p1} = W(\xi^o, \eta^o)$, eq. (2.21) can be obtained from $W^{o1}/2$ by replacing $\underline{\xi}^1$ with $\underline{\xi}^o$. Because of eqs. (B8) there is no contribution from the separation line(s) while this time the plasma boundary contributes. Thus, eq. (2.21) is obtained from eq. (B5) by the replacements $W^{o1}/2 \to \text{Min}\delta W_{p1}$, $(\underline{n} \cdot \underline{\xi}^1) \to \xi_n$ and by connecting the line integrals over the sections of the boundary. Again with eq. (2.13b) in the non-doublet region the case $\xi_n = \xi_n^a$ is properly included.

b) We now show that the system of differential equations (2.13) and (2.19) coupled by the boundary conditions required in Section II has a unique solution. We consider only the case with two doublet regions, the case with one being quite analogous.

Let us define the arc length to the upper end of the separation lines

by

$$l_r = l(R_r) \quad , \qquad l_l = l(R_l) \quad . \tag{B9}$$

Because of $\hat{\dot{R}}(l_r) = \hat{\dot{R}}(l_l) = 0$, two terms in eq. (2.19) diverge at the separation lines, and, equating them, with $\hat{\dot{z}}(l_r) = -\hat{\dot{z}}(l_l) = 1$ and $\hat{z}(l_r) = \hat{z}(l_l) = 0$ we obtain

$$\dot{f}(l_r) = \dot{f}_r = \frac{4}{\gamma^2}\,\hat{\xi}_n(l_r)\,\dot{R}(l_r), \qquad \dot{f}(l_l) = \dot{f}_l = -\frac{4}{\gamma^2}\,\hat{\xi}_n(l_l)\,\dot{R}(l_l) \quad . \tag{B10}$$

In the case $\xi_n = \xi_n^a$ we have $\hat{\xi}_n^a(l_r) = \hat{\xi}_n^a(l_l) = 0$ and with eqs. (B10) this proves that the conditions in eq. (2.14a) are automatically satisfied, as shown in appendix A. Since in this case $f(l) \equiv 0$ in the non-doublet region, the continuity requirement for $\dot{f}(l)$ across the separation lines is already satisfied.

In the case $\xi_n = \xi_n^s$ it leads to the boundary value problem

$$\ddot{f} + a\,\dot{f} + b\,f = i \quad ; \quad \dot{f}(l_r) = \dot{f}_r \quad , \quad \dot{f}(l_l) = \dot{f}_l \tag{B11}$$

in the non-doublet region, where a,b and i are short notations for the coefficients of eq. (2.13a). Note that we have

$$b < 0 \quad . \tag{B12}$$

We introduce two solutions f_h^1 and f_h^2 of the initial value problems

$$\begin{aligned} \dot{f}_h^1(l_r) &= 0, & f_h^1(l_r) &= 1 \\ \dot{f}_h^2(l_l) &= 0, & f_h^2(l_l) &= 1 \end{aligned} \tag{B13}$$

for the corresponding homogeneous differential equation and an arbitrary special solution f_i of the inhomogeneous one. As shown, for example, in the Appendix of Ref. [2], it follows from inequality (B12) that

$$\dot{f}_h^1(1_1) \neq 0, \qquad \dot{f}_h^2(1_r) \neq 0 \ . \tag{B14}$$

Inserting the general solution $f = f_i + c_1 f_h^1 + c_2 f_h^2$ into the boundary conditions (B10) yields a system of two linear equations for c_1 and c_2 with nonvanishing coefficient determinant because of (B14), and thus for the non-doublet region a unique solution $f(1)$ is obtained. We denote its values at the endpoints by

$$f(1_r) = f_r \ , \qquad f(1_1) = f_1 \ . \tag{B15}$$

Let us now turn to the doublet regions, and for simplicity consider only the right one. The two cases $\xi_n = \xi_n^a$ and $\xi_n = \xi_n^s$ can be treated simultaneously. We introduce

$$1_m = 1(R_{max}) \ . \tag{B16}$$

Since $f(1)$ must be continuous at 1_r and since at 1_m we have the condition (2.20), we must now consider the problem

$$\ddot{f} + a\dot{f} + bf = i \ ; \quad \dot{f}(1_m) = 0, \quad f(1_r) = f_r, \tag{B17}$$

where a,b and i are the coefficients of eq. (2.19) and $f(1)$ has to be determined in the interval $0 \leq 1 \leq 1_r$.

Connecting at 1_m solutions of initial value problems in $1_m \geq 1 \geq 0$

and $l_m \leq l \leq l_r$ we temporarily introduce a solution f_h of the homogeneous and a solution f_i of the inhomogeneous problem which satisfies

$$f_h(l_m) = \dot{f}_h(l_m) = f_i(l_m) = \dot{f}_i(l_m) = 1 \quad . \tag{B18}$$

For both we construct "conjugate" solutions

$$\hat{f}_h(l) = f_h(\hat{l}) \ , \qquad \hat{f}_i(l) = f_i(\hat{l}) \quad . \tag{B19}$$

Writing down eq.(2.19) at the conjugate point it is seen that $\hat{f}_h(l)$ and $\hat{f}_i(l)$ are also solutions of the homogeneous and inhomogeneous differential equations respectively. Obviously, we have

$$\hat{f}_h(l_m) = -\dot{\hat{f}}_h(l_m) = \hat{f}_i(l_m) = -\dot{\hat{f}}_i(l_m) = 1 \tag{B20}$$

and hence $\hat{f}_h(l)$ and $f_h(l)$ are linearly independent.
The two homogeneous solutions derived from them

$$f_h^s = \frac{1}{2}\,(f_h + \hat{f}_h), \quad f_h^a = \frac{1}{2}\,(f_h - \hat{f}_h) \tag{B21}$$

and the special inhomogeneous solution

$$f_i^s = \frac{1}{2}\,(f_i + \hat{f}_i) \tag{B22}$$

derived from f_h, $\hat{f}_h$ and f_i, $\hat{f}_i$ have the properties

$$\dot{f}_h^s(l_m) = \dot{f}_i^s\,(l_m) = 0, \quad \dot{f}_h^a\,(l_m) = 1 \ , \tag{B23}$$

and the most general inhomogeneous solution which satisfies the first of the boundary conditions (B17) is

$$f = f_i^s + c_s f_h^s \tag{B24}$$

Using the fact that also the coefficient b in the diff. eq. (B17) is negative, it can again be shown that

$$\dot{f}_h^s(1) > 0 \quad \text{for} \quad 1 > 1_m. \tag{B25}$$

From this and $f_h^s(1_m) = 1$ we get $f_h^s(1_r) \neq 0$ and the coefficient c_s in the solution (B24) may thus be uniquely determined from the second boundary condition (B17).

We note that the different solutions of initial value problems employed above exist according to standard mathematical theorems, and thus the existence and uniqueness of the functions f(1) is proven. It follows immediately from eqs.(B21) and (B22) that the solution (B24) satisfies the condition

$$\hat{f(1)} = f(1) ,$$

i.e. it defines a single-valued function f(R) = f(1(R)). In the non-doublet region the problem of multi-valuedness does not arise, so that finally the unique single-valued existence of the Euler solutions is demonstrated.

References

[1] REBHAN, E., SALAT, A., Nucl. Fusion 16 (1976) 805.

[2] REBHAN, E., SALAT, A., Nucl. Fusion 17 (1977) 251.

[3] FREIDBERG, J.P., GROSSMANN W., Phys. Fluids 18 (1975) 1494

[4] CHU, M.S., DOBROTT, D.R., GUEST, G.E., HELTON, F.J., JENSEN, T.H., LUXON, J.L., MILLER, R.L., OHKAWA, T., RAWLS, J.M., WANG, T.S., WESLEY, J.C., General Atomic Report GA - A14092 (1977); in Plasma Physics and Controlled Nuclear Fusion Research (Proc. 6th. Int. Conf. Berchtesgaden, 1976) Nucl. Fusion Supplement, II, (1977) 387.

[5] DOBROTT, D.R., MILLER, R.L., Phys. Fluids 20 (1977) 1361

[6] CHU M.S., MILLER, R.L., General Atomic Report GA - A14323 (1977).

Figure captions

Fig. 1 Stability diagram in an ε-β plane with boundary for axisymmetric stability ($n=0$) according to Rebhan, Salat, in Ref. [2] (vertical straight line) and for nonaxisymmetric stability ($n\neq 0$) according to Freidberg, Grossmann, in Ref. [3], stable region shaded.

Fig. 2 Doublet cross-section with coordinates.

Fig. 3 Minimizing antisymmetric perturbations (unstable) in a typical doublet-type plasma with $A = 3$, $\beta_p = 1$, $q = 1$.

Fig. 4 Two-dimensional analogue of the optimization procedure, path through parameter space dotted.

Fig. 5 Optimum shapes depending on A
a) for $q = 1$, $\beta_p = 1$ b) for $q = 1$, $\beta_p = 2$,
axis of symmetry to the left.

Fig. 6 Test of the maximum property of W_{min} for the optimum shape at $A = 5$, $\beta_p = 1$, $q = 1$. All quantities are normalized with their values at optimum position.

Fig. 7 Constricted doublet-type cross-sections obtained for $A < A^*$ at intermediate steps of the optimization procedure
a) for $\beta_p = 1$ and b) for $\beta_p = 2$,
axis of symmetry to the left.

Fig. 8 ß enhancement over circular shape as a function of A for the optimum shapes with $A \geq A^*$ and the intermediate shapes with $A < A^*$ of Figs. 7a) and b)

Fig. 9 ß enhancement of optimum shapes and elliptical shapes for $ß_p = 1$.

Table 1: Fourier coefficients, eq. (1.8), of optimum shapes for $ß_p = 1$ and several values of A.

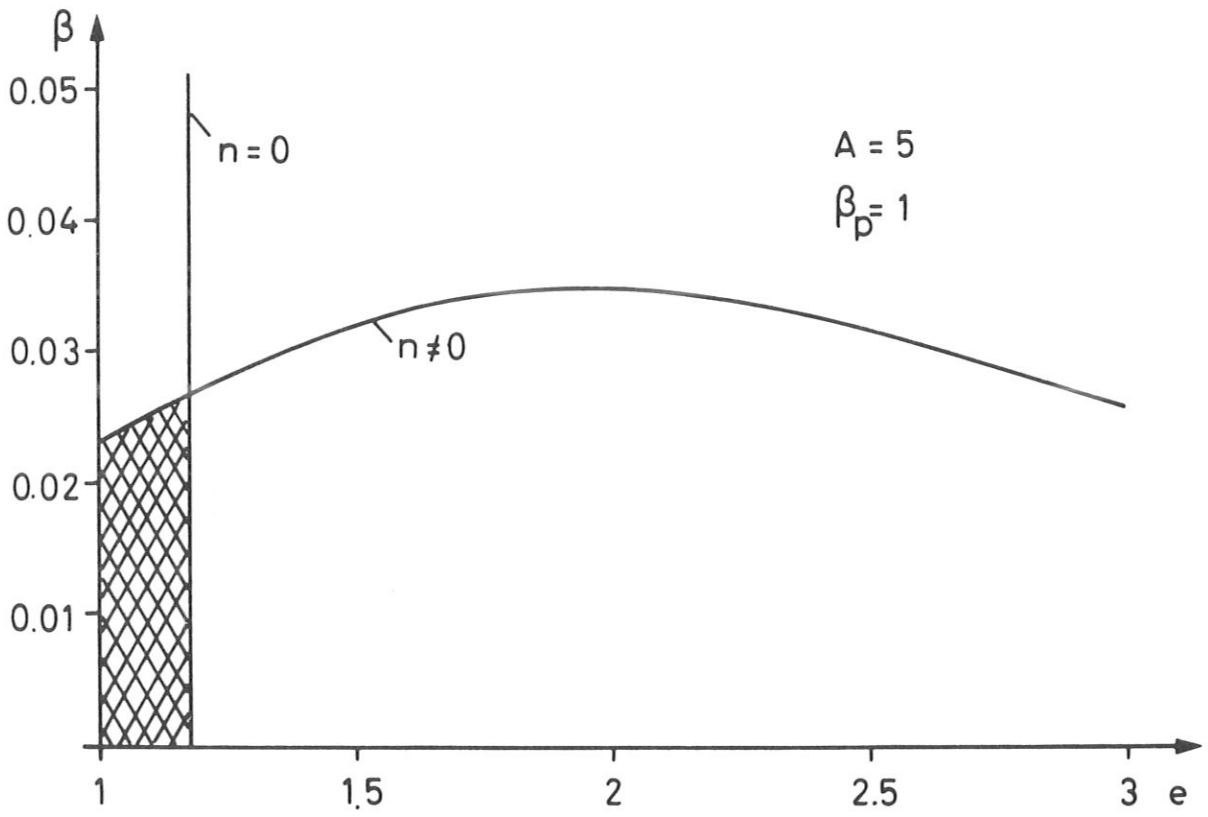

Fig. 1 Stability diagram in an e-ß plane with boundary for axisymmetric stability (n = 0) according to Rebhan, Salat, in Ref. [2] (vertical straight line) and for nonaxisymmetric stability (n ≠ 0) according to Freidberg, Grossmann in Ref. [3], stable region shaded.

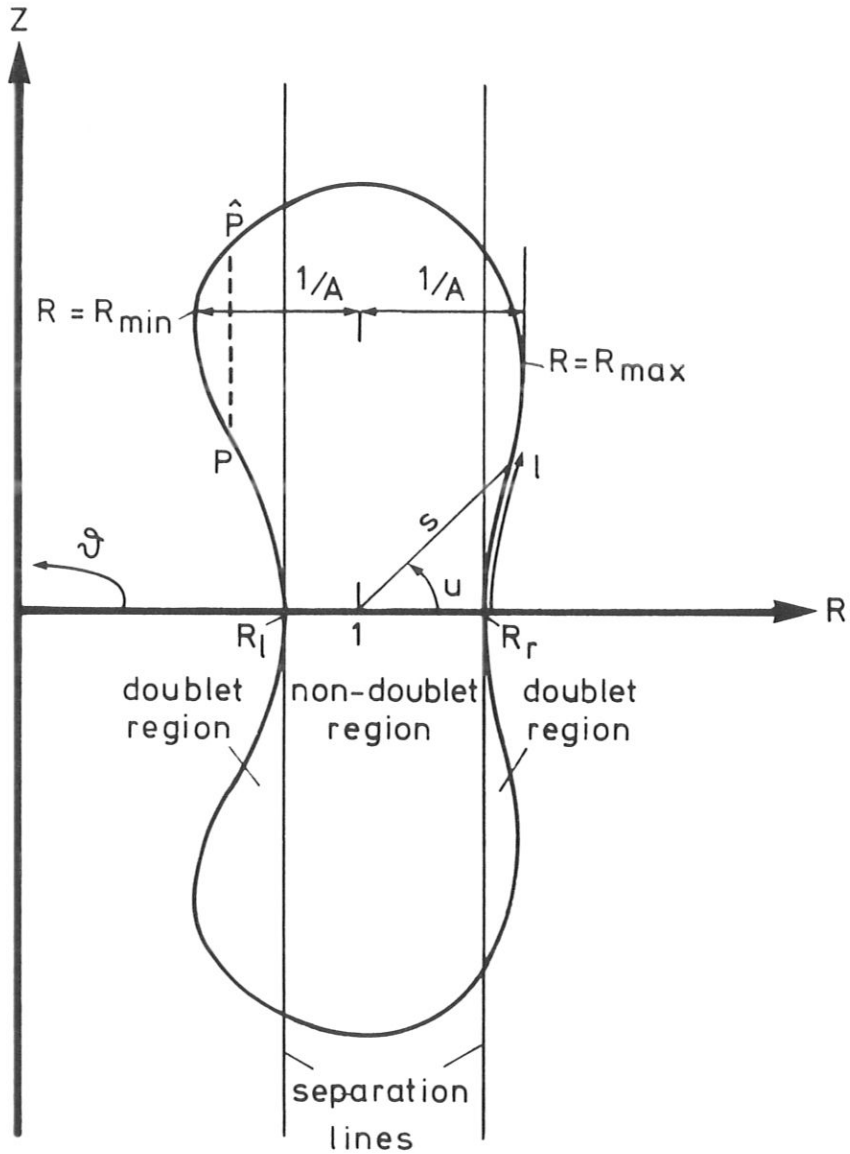

Fig. 2 Doublet cross-section with coordinates.

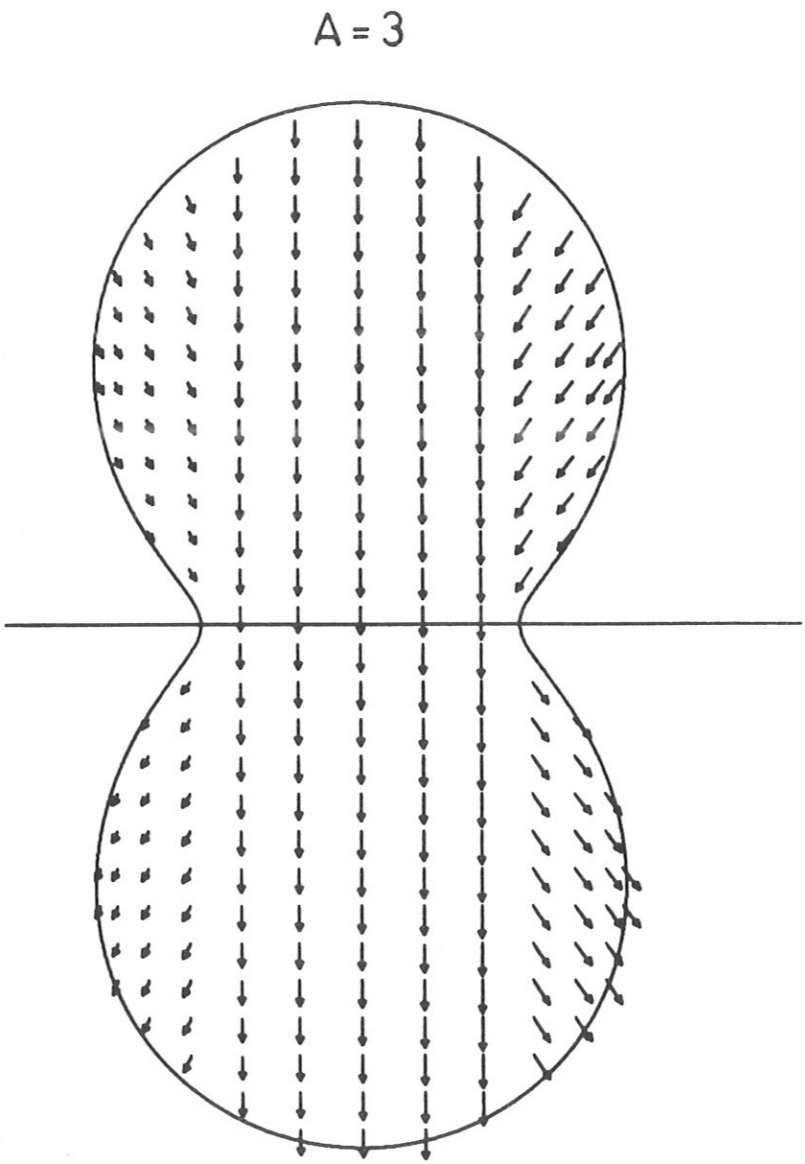

Fig. 3 Minimizing antisymmetric perturbations (unstable) in a typical doublet-type plasma with $A = 3$, $\beta_p = 1$, $q = 1$.

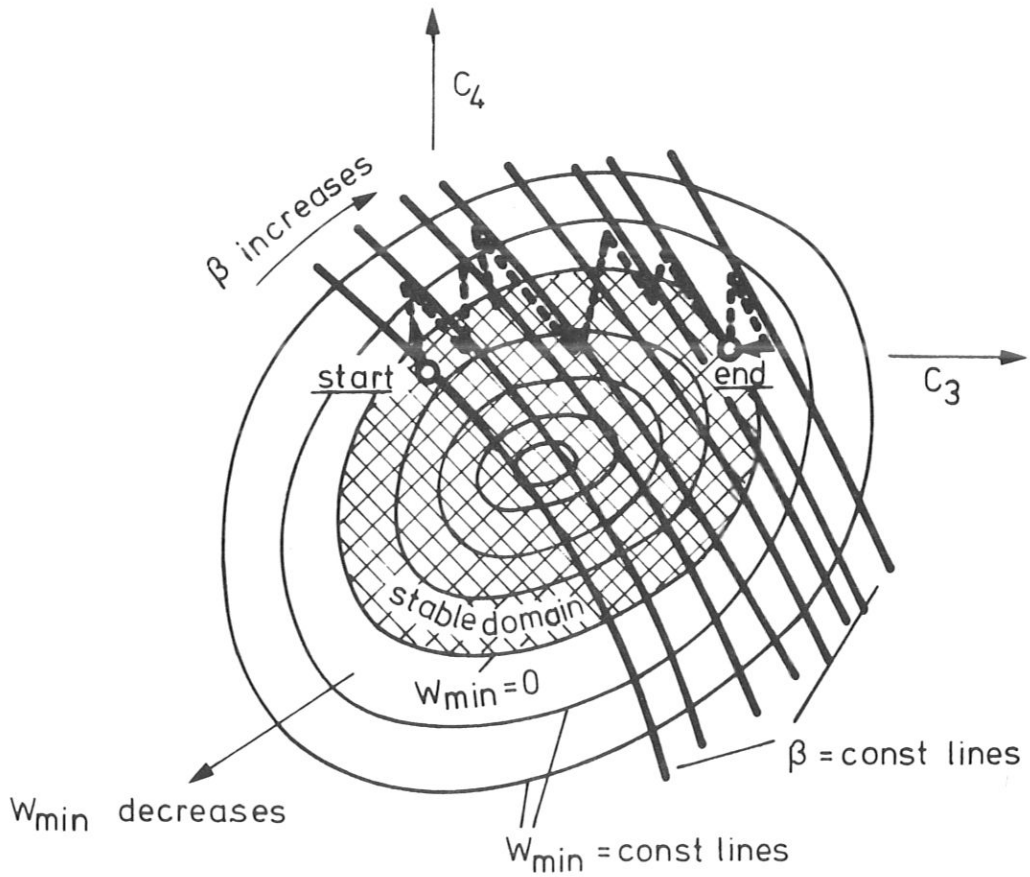

Fig. 4 Two-dimensional analogue of the optimization procedure, path through parameter space dotted.

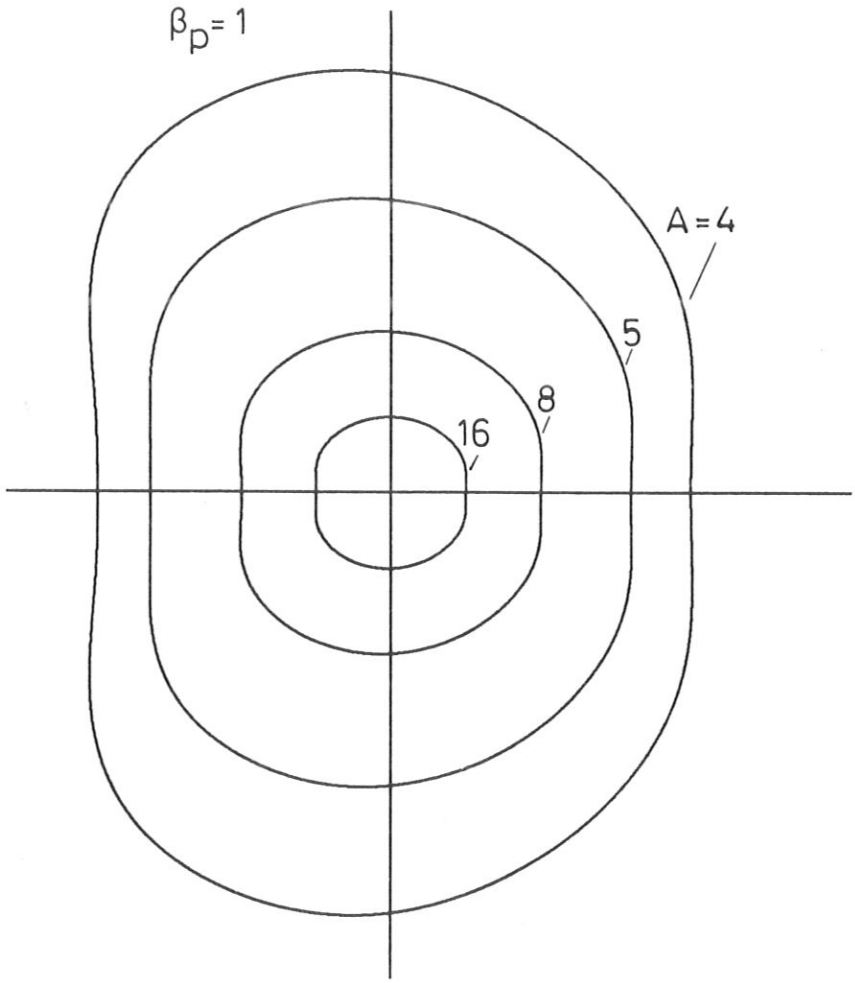

a)

Fig. 5 Optimum shapes depending on A

a) for q = 1, β_p = 1 b) for q = 1, β_p = 2,

axis of symmetry to the left.

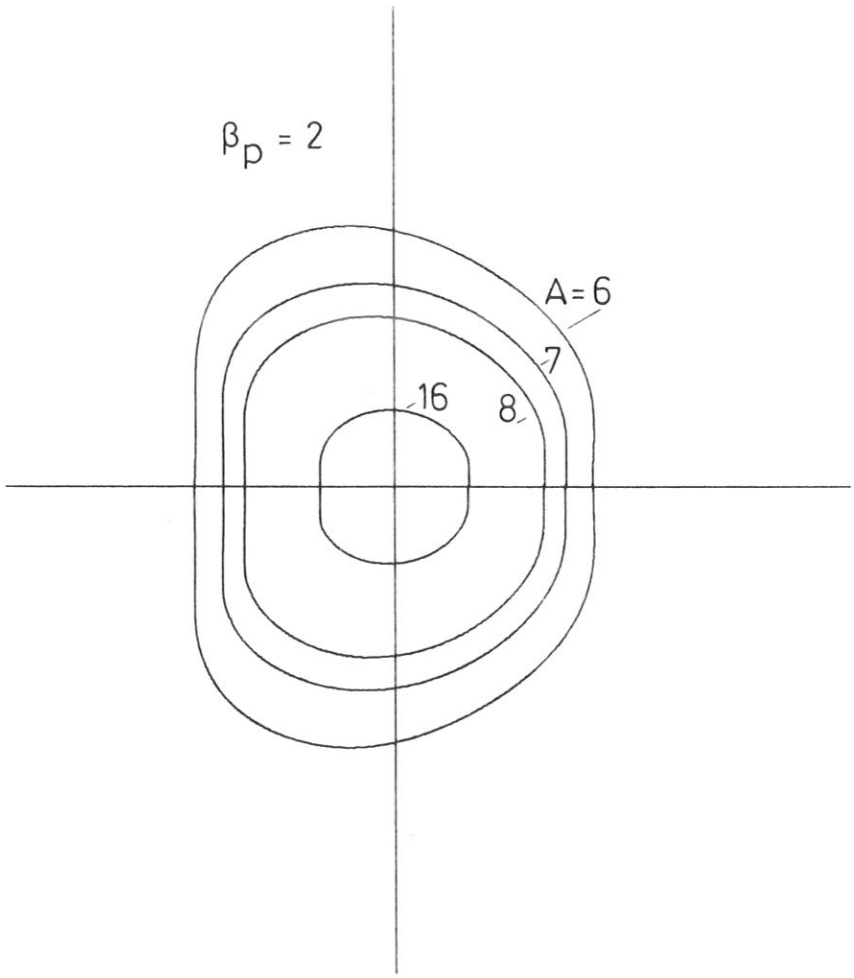

b)

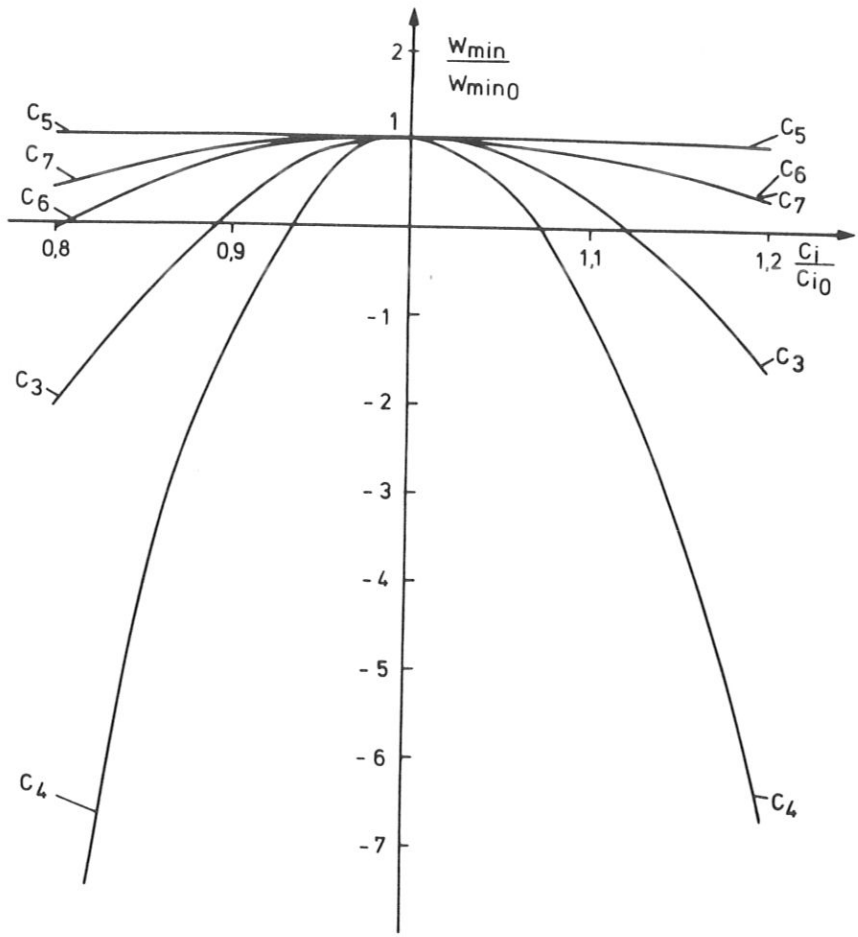

Fig. 6 Test of the maximum property of W_{min} for the optimum shape at A = 5, β_p = 1, q = 1. All quantities are normalized with their values at optimum position.

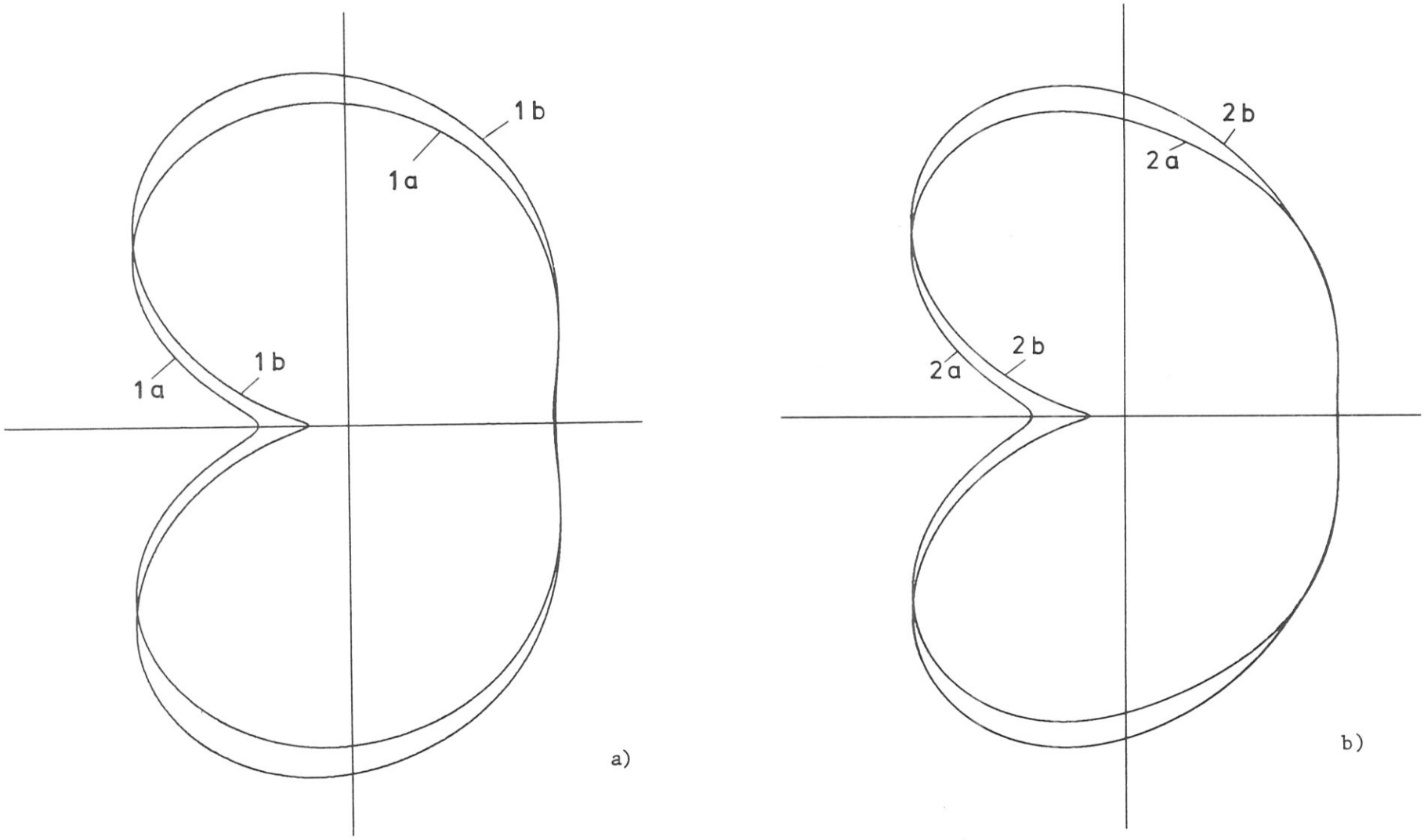

Fig. 7 Constricted doublet-type cross-sections obtained for $A < A^*$ at intermediate steps of the optimization procedure a) for $\beta_p = 1$ and b) for $\beta_p = 2$, axis of symmetry to the left.

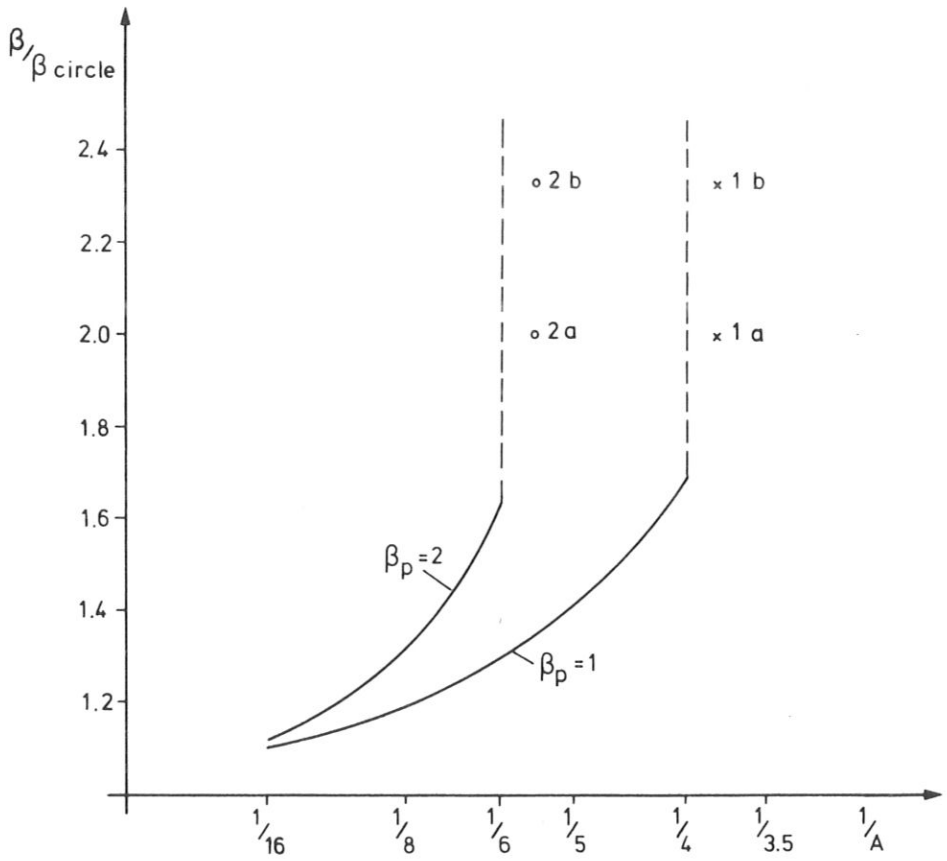

Fig. 8 ß enhancement over circular shape as a function of A for the optimum shapes with $A \geq A^*$ and the intermediate shapes with $A < A^*$ of Figs. 7a) and b)

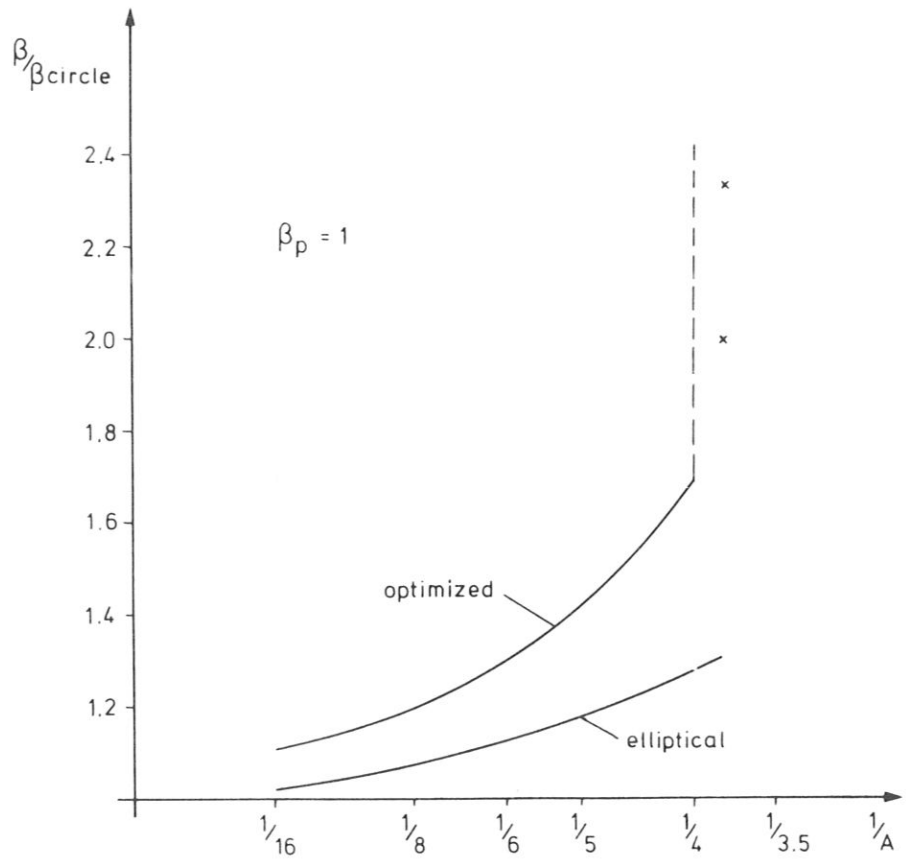

Fig. 9 ß enhancement of optimum shapes and elliptical shapes for $ß_p = 1$.

Table 1

A	16	8	4	3.8 a	3.8 b
c	$6.5 \cdot 10^{-2}$	$1.3 \cdot 10^{-1}$	$3.1 \cdot 10^{-1}$	$3.2 \cdot 10^{-1}$	$3.3 \cdot 10^{-1}$
c_1	$-9.1 \cdot 10^{-3}$	$-1.6 \cdot 10^{-2}$	$-2.2 \cdot 10^{-2}$	$7.4 \cdot 10^{-2}$	$1.2 \cdot 10^{-1}$
c_2	$1.5 \cdot 10^{-3}$	$-3.1 \cdot 10^{-2}$	$-1.7 \cdot 10^{-1}$	$-3.2 \cdot 10^{-1}$	$-4.2 \cdot 10^{-1}$
c_3	$8.6 \cdot 10^{-3}$	$1.8 \cdot 10^{-2}$	$4.1 \cdot 10^{-2}$	$1.1 \cdot 10^{-1}$	$1.5 \cdot 10^{-1}$
c_4	$-2.5 \cdot 10^{-2}$	$-3.0 \cdot 10^{-2}$	$-3.2 \cdot 10^{-2}$	$-8.6 \cdot 10^{-2}$	$-9.3 \cdot 10^{-2}$
c_5	$2.6 \cdot 10^{-3}$	$3.9 \cdot 10^{-3}$	$-5.0 \cdot 10^{-3}$	$3.6 \cdot 10^{-2}$	$3.6 \cdot 10^{-2}$
c_6	$-1.3 \cdot 10^{-2}$	$-1.2 \cdot 10^{-2}$	$-1.2 \cdot 10^{-4}$	$-2.3 \cdot 10^{-2}$	$-1.8 \cdot 10^{-2}$
c_7	$2.2 \cdot 10^{-5}$	$-1.9 \cdot 10^{-4}$	$-5.6 \cdot 10^{-3}$	$9.1 \cdot 10^{-3}$	$9.1 \cdot 10^{-3}$
c_8	$-4.4 \cdot 10^{-3}$	$-3.7 \cdot 10^{-3}$	$4.2 \cdot 10^{-3}$	$-4.9 \cdot 10^{-3}$	$-3.0 \cdot 10^{-3}$